ELSEVIER

PII: S0032-3861(97)00554-5

Polymer Vol. 39 Nos. 6–7, pp. 1405–1414, 1998

0032-3861/97/$17.00+0.00

The (010)–(120) crystal growth face transformation in poly(ethylene oxide) spherulites

J. M. Marentette† and G. R. Brown*
Department of Chemistry, McGill University, 801 Sherbrooke Street West, Montreal, Quebec, Canada, H3A 2K6
(Received 27 March 1996; revised 20 January 1997)

The crystallization and melting of poly(ethylene oxide) (PEO) have been examined in detail using polarized light microscopy (PLM), polarized infrared microspectroscopy (PIRM) and differential scanning calorimetry (DSC). Examination of the orientation of the crystalline stems within the spherulites by PIRM supports the hypothesis that the dominant crystal growth face of PEO changes from the (010) crystallographic plane at crystallization temperatures (T_c) $< 51°C$ to the (120) plane at $T_c > 51°C$. The cusp in the logarithmic growth rate–temperature plot appears to be the result of this phenomenon. Analysis of spherulitic growth rate data for the monodisperse sample ($M_w = 1.8 \times 10^5$) fails to provide evidence in support of the regime II/III transition proposed in a previous literature study and indicates that in the range 45–56°C crystallization occurs solely within regime III. The larger value for the product of the lateral and fold surface free energies in the case of (010) growth appears to arise from the higher fold surface free energy of this growth face. The difference in the fold surface free energies of the different growth faces, 41 erg/cm^2 for the (010) face as compared with 29 erg/cm^2 for the (120) face, can be accounted for by the corresponding differences in the minimum chain length required for chain folding in the case of adjacent re-entry.

(Keywords: PEO crystallization; infrared microspectroscopy; regimes)

INTRODUCTION

The thermal properties, crystalline morphology and crystallization kinetics of poly(ethylene oxide), PEO, have commanded much attention during the past three decades. A significant portion of the crystallization temperature range of PEO is experimentally accessible, and at low to intermediate supercoolings crystallization from the melt yields large, distinct spherulites ($> 100\ \mu m$ in diameter) that are easily observed in thin section using polarized light microscopy (PLM). As a result, the crystallization kinetics and morphology of PEO spherulites have been examined in the pure state[1–13] as well as in numerous blends with other polymers[14–21]. Yet there remain fundamental questions regarding the crystallization and melting of this polymer. For example, a wide range of values for the equilibrium melting temperature (T_m^o) are quoted in the literature[22,23]. This question, in particular, is of direct relevance to the identification of regime transitions, as indicated by the analysis of spherulite growth rate as a function of crystallization temperature, T_c.

Of primary interest is the occurrence of a regime II/III transition at ~51°C in low to intermediate molecular weight PEO reported by Cheng *et al.*[1]. An X-ray diffraction study of spherulitic films of low molecular weight PEO, conducted subsequently by Point *et al.*[24], demonstrated that the dominant crystal growth face in such films changes from the (010) crystallographic plane at crystallization temperatures $< 50°C$ to the (120) plane at temperatures between 50 and 58°C. This led them to question the occurrence of a regime II/III transition at ~51°C. According to the authors of the latter study, the possibility of such a growth face transformation in PEO spherulites is of particular relevance to the interpretation of spherulite crystallization kinetics data due to the assumption of current nucleation theory that the identity of the dominant growth face is conserved in the different crystallization regimes[25–27]. Specifically, it was proposed[24] that a change in the dominant growth face at a given crystallization temperature (T_c) precludes the possibility of a regime transition at the same T_c. However, no further scrutiny of crystallization kinetics data was presented, and it is not clear that a regime transition could not occur simultaneously with a transformation in the dominant growth face, particularly in light of the results of previous studies of *cis*-polyisoprene (c-PI)[28,29]. *Cis*-polyisoprene crystallizes as two distinct types of spherulitic structures, each possessing characteristic growth rates, lamellar thicknesses and dominant growth faces[29]. In the so-called 'α' form the growth direction corresponds to the crystallographic *a*-axis; while in the 'β' form the *b*-axis is the growth direction. One of the crystal forms has been found to exhibit one or two regime transitions, depending on the molecular weight of the sample[28].

In the investigation described in this paper, the conventional technique of polarized light microscopy was coupled with the novel technique of polarized infrared microspectroscopy to examine the microstructure of specific areas of PEO spherulites at the level of the

* To whom correspondence should be addressed at: University of Northern British Columbia, Chemistry Programme, 3333 University Way, Prince George, BC, Canada V2N 4Z9
† Present address: Max Planck Institute for Polymer Research, Ackermann-weg 10, Postfach 3148, D-55021 Mainz, Germany.

individual crystalline stems for additional evidence of a growth face transformation. Spherulite radial growth rates for the temperature region of interest were acquired and are examined in detail. Differential scanning calorimetry was employed to obtain the required melting temperature data.

EXPERIMENTAL

Synthesis

Monodisperse PEO was synthesized by anionic polymerization using diphenylmethyl potassium as the catalyst and tetrahydrofuran (THF) as the solvent. It was dissolved in toluene and precipitated by slow addition of an excess of hexanes at room temperature to remove low molecular weight contaminants. The resultant white powder was then dried under vacuum at room temperature for 4 weeks prior to initial crystallization measurements. Due to the adverse effect of water or other solvents on the crystallization kinetics[30], the polymer was stored under vacuum.

Gel permeation chromatography, using a Varian DS-600 Chromatograph equipped with Waters Ultrastyragel columns (THF mobile phase) and interfaced with a Varian RI-4 Refractive Index Detector, indicated a weight average molecular weight, M_w, of 1.8×10^5 with a polydispersity, $M_w/M_n = 1.4$ relative to polystyrene standards.

Polarized light videomicroscopy

Thin sections of PEO (~20 μm thickness, ~5 mm diameter) were prepared by placing a small amount (~1 mg) of powder on a circular, glass coverslip (0.1 mm thickness, 13 mm diameter) and melting the sample at 100°C. Aluminum shims (15 μm thickness) were positioned on either side of the sample. Light pressure was applied to the molten sample to ensure uniform sample spreading. Samples were cooled at room temperature for a minimum of 30 min before use. The apparatus and techniques used to determine the growth rates of spherulites were similar to those described in previous reports from this laboratory[31,32].

Preliminary experiments showed that at a premelting temperature of 100°C, a premelting time of 2 min was required to erase the thermal history of a sample. The molten sample was cooled from 100 to 45°C at 130°C/min for spherulite nucleation, then allowed to equilibrate at the selected T_c in the range 45–56°C. Separate experiments confirmed that the choice of nucleation temperature did not influence the crystallization kinetics or morphology at T_c[30]. Thin sections were melted and recrystallized up to six times with no effect on radial growth rates.

Infrared microspectroscopy

Thin sections (20 μm) were prepared between Teflon sheets to minimize the potential of introducing strain or damaging the spherulites during removal of samples from their substrates (Ref. 30 gives details). The premelting temperature of the hotplate was 110°C, and the premelting time was 5 min. Times were chosen to permit complete crystallization at the selected T_c. The samples were stored in a dessicator, at room temperature, for no longer than 24 h prior to acquisition of spectra.

Spectra were acquired using a Perkin-Elmer Infrared Microscope equipped with a fixed 100 μm diameter aperture and a mercury–cadmium–telluride (MCT) detector, and interfaced with a Perkin-Elmer 16PC Infrared Spectrometer and a personal computer. A thin section was placed between KBr plates (13 mm diameter, 1 mm thick) to ensure that the sample remained flat during the experiment. The sample was viewed between crossed, visible light polaroid sheets to locate areas ~200 μm from spherulite centres for data acquisition. Two or three areas were selected in each of a minimum of three thin sections crystallized at each T_c. At each location 'parallel' and 'perpendicular' spectra were recorded with the infrared polarizer oriented tangentially and radially relative to the spherulite geometry, respectively. A 'background' spectrum of 16 scans at a resolution of 2 cm^{-1} was acquired prior to each 'sample' spectrum, and a total of 32 scans were accumulated for each sample spectrum.

To obtain a spectrum of amorphous PEO at 100°C, the infrared microscope stage was modified to enable attachment of a Mettler FP52 Microscope Hotstage interfaced with an FP5 Temperature Controller. A thin section of PEO mounted between KBr plates was heated at a rate of 1°C/min to 100°C and allowed to equilibrate for 2 min. A background spectrum of 32 scans was acquired at 100°C prior to acquisition of a sample spectrum of 128 scans.

Differential scanning calorimetry

The melting behaviour was studied with a Perkin-Elmer DSC-7 calibrated according to procedures described previously[31]. Each sample (weighing 5.0 ± 0.2 mg) was held in the melt at 100°C for 15 min, then quenched at a nominal rate of 200°C/min to the selected T_c. The sample was maintained at T_c for 24 h or, in the instance of very low supercooling, a length of time sufficient to ensure complete crystallization, then heated at 10°C/min to 100°C.

RESULTS AND DISCUSSION

Spherulite morphology

The birefringence and morphology of PEO spherulites have been discussed in detail in the literature[33–35]. At intermediate supercooling, i.e. at T_c between 40 and 51°C, PEO crystallizes as negatively birefringent spherulites that exhibit a distinct Maltese cross extinction pattern (*Figure 1a*). As the supercooling is decreased to temperatures approaching 51°C, the spherulite structure becomes coarser, or looser, and the birefringence becomes more step-like (*Figure 1b*); however, the sign of the birefringence is conserved. The spherulite shown in *Figure 1c* was nucleated at 40°C and allowed to grow for ~120 μm (radius) before the temperature was rapidly increased to 55°C, where the sample was allowed to crystallize isothermally for an additional 50 μm. The centre of the spherulite exhibits the typical, well-defined birefringence pattern of the lower crystallization temperature, but the regions of the spherulite farthest from the centre exhibit a very diffuse, mixed morphology.

There is a gradual evolution of spherulite structure from a tight, closed structure with a well-defined Maltese cross when viewed using crossed polars at $T_c < 51$°C to an open, mixed structure at $T_c > 51$°C. These textural changes have previously been associated with a proposed regime II/III transition[1]. Few correlations between significant changes in spherulite morphology and regime transitions have been reported to date. For example, studies involving isotactic polypropylene[36] (i-PP) and poly(phenylene sulfide)[37] failed to reveal morphological changes that coincided with regime transitions; however, the polydispersity of these samples may have masked morphological transitions. On the other hand, polyethylene (PE) undergoes a morphological transition from axialitic structures in regime I to regular

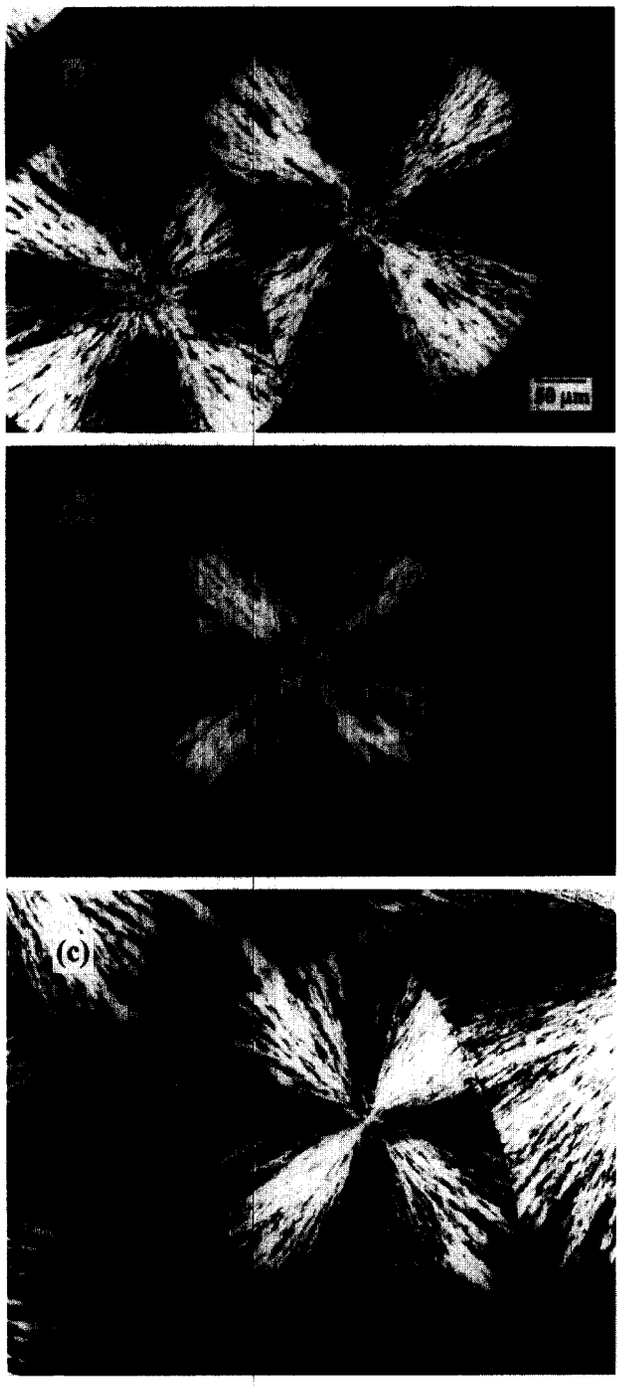

Figure 1 PEO spherulite morphology at various T_c: (a) 45°C; (b) 49°C and (c) T_n 40°C − T_c 55°C

spherulites in regime II[38]. A similar correlation has been described in the case of c-PI[28].

Crystalline microstructure: stem orientation

The ability to obtain polarized spectra of small, selected areas of thin samples makes polarized infrared microspectroscopy (PIRM) ideally suited to the analysis of crystallite orientation within spherulites, an application that has not been reported to date in the literature. To describe the degree of sample orientation, use is made of the dichroic ratio, R, defined as

$$R = \frac{A_{\parallel}}{A_{\perp}} \tag{1}$$

where the subscripts $\parallel$ and $\perp$ denote parallel and perpendicular orientation relative to the reference direction, respectively. Typically, the parallel direction of drawn samples is the draw direction or the direction of the polymer chain axes, and the perpendicular direction lies perpendicular to the chain axes[39]. In the present study of spherulites, the radial direction is designated as the 'perpendicular' direction, and the tangential direction is designated as the 'parallel' direction. Throughout the following discussion, a spectrum acquired with the infrared polarizer oriented parallel to the spherulite radius is referred to as a 'perpendicular spectrum'; while a spectrum acquired with the polarizer oriented along the tangential direction of the spherulite is referred to as a 'parallel spectrum'. Because the parallel direction does not coincide with the length of the chain axes, the magnitude of the dichroism observed in spherulitic thin sections is less than that observed in oriented samples, such as drawn fibres, composed of the same material. However, spherulitic dichroic ratio measurements provide a measure of the degree and nature of the orientation found in sub-spherulitic structure.

To obtain spectra of purely crystalline PEO, the original spectra were refined by removal of the contribution arising from the amorphous component. For example, the parallel and perpendicular spectra of PEO crystallized at 49°C, shown in *Figure 2a* and *Figure 3a*, were refined to yield the purely crystalline spectra in *Figure 2b* and *Figure 3b* by subtraction of the melt spectrum of PEO, shown in *Figure 4*, using the appropriate scaling factor[30]. The dichroism of the various vibrations of spherulitic PEO at $T_c = 49$°C coincides with the dichroism of the vibrations of oriented, fibrous PEO reported in the literature[40]. The vibrations at 1468, 1360, 1281, 1062 and 843 cm^{-1} are perpendicular to the chain axis, while the vibrations at 1455, 1344, 1243, 965 and 947 cm^{-1} are parallel to the chain axis, as indicated by dichroic ratios less than and greater than unity, respectively. According to the literature vibrational assignments[40], the parallel bands generally correspond to unique vibrations, whereas the perpendicular bands correspond to a combination of two different vibrations.

Figure 5 illustrates the orientations of the unit cell in samples crystallized at temperatures above and below the growth face transition temperature of 51°C as proposed by Point *et al.*[24]. While crystallization with the (010) face as the growth front, i.e. with the crystallographic b-axis as the radial direction, results in chain axes that are perpendicular to the plane of the spherulite, crystallization with the (120) face as the growth front leaves the chain axes perpendicular to the plane of the spherulite, but causes the helices to be rotated ~45° about the c-axis. According to this model the perpendicular vibrations that are oriented radially when the (010) face is the dominant growth face acquire a significant parallel component when the (120) face becomes dominant. Because the shift in the radial direction is 45°, vibrations that are predominantly radial in the case of a (010) growth face acquire an orientation that is intermediate between radial and tangential orientations in the case of a (120) growth face. Therefore, in the latter case the dichroic ratios of the perpendicular modes are expected to be intermediate between parallel and perpendicular orientation, i.e. the values of R should approach unity. Because the parallel modes are oriented mainly along the chain axes, which lie perpendicular to the plane of the spherulite, the corresponding values of R are not expected to approach unity as closely as in the case of the perpendicular modes.

Figure 6 reveals the two dominant trends exhibited by the dichroic ratio data with increasing T_c. The perpendicular modes at 1360 and 1281 cm^{-1} show little or no change from

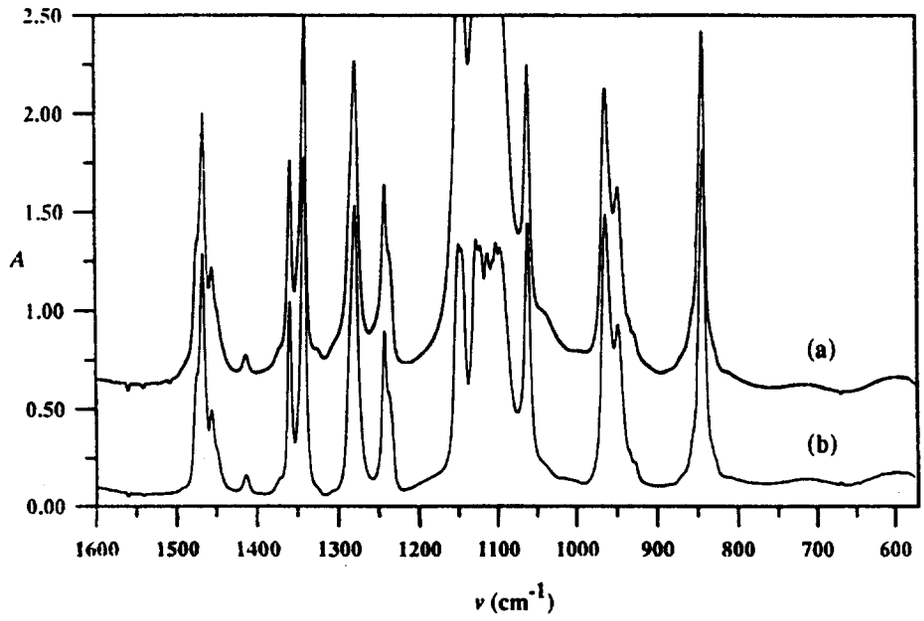

Figure 2 Dichroic spectra of PEO, $T_c = 49°C$: parallel spectrum (a) before and (b) after subtraction of the amorphous component of PEO

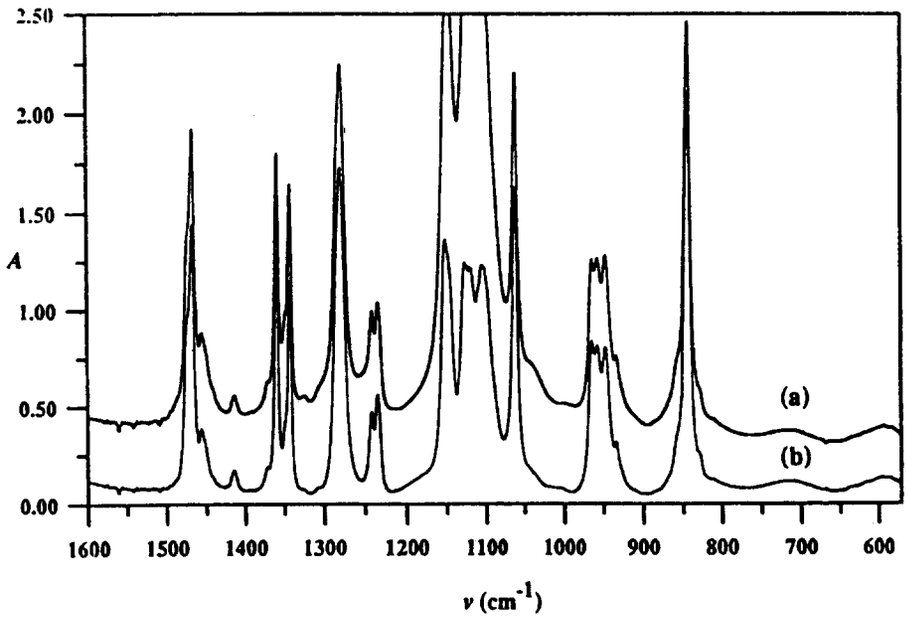

Figure 3 Dichroic spectra of PEO, $T_c = 49°C$: perpendicular spectrum (a) before and (b) after subtraction of the amorphous component of PEO

49 to 53°C; however, for these modes the value of R increases to ~1.0 at 55°C. The parallel bending mode at 1455 cm^{-1} and the rocking mode at 965 cm^{-1} exhibit pronounced changes, as expected in the instance of a (010)–(120) growth face transformation for modes involving motions perpendicular to the chain axes, or in the plane of the spherulite. This behaviour is, in part, complementary to that of the perpendicular modes; that is, R decreases towards unity with increasing T_c. These trends in the dichroic ratio data are consistent with a (010)–(120) growth face transformation and the concomitant change in the orientation of the crystalline chain axes at ~51°C.

Spherulite crystallization kinetics

In view of the apparent growth face transformation at ~51°C, the radial growth rates of PEO spherulites merit further investigation. Therefore, spherulitic growth rate data were obtained and examined with particular attention to the T_c range in the vicinity of 51°C. Current nucleation theory, as developed by Hoffman, Davis, Lauritzen and Miller[25–27], describes the growth rate of spherulites using the following expression

$$G = G_o \exp\left[\frac{-U^*}{R(T_c - T_\infty)}\right] \exp\left[\frac{-K_g}{T_c(\Delta T)f}\right] \quad (2)$$

where G_0 is a pre-exponential factor, U^* is the activation energy for reptation in the melt, R is the ideal gas constant, T_∞ is the temperature of cessation of molecular motion (often taken as $T_g - 30$ K), and ΔT is the supercooling, $T_m^o - T_c$. The dimensionless correction factor, f,

$$f = \frac{2 \cdot T_c}{T_m^o + T_c} \quad (3)$$

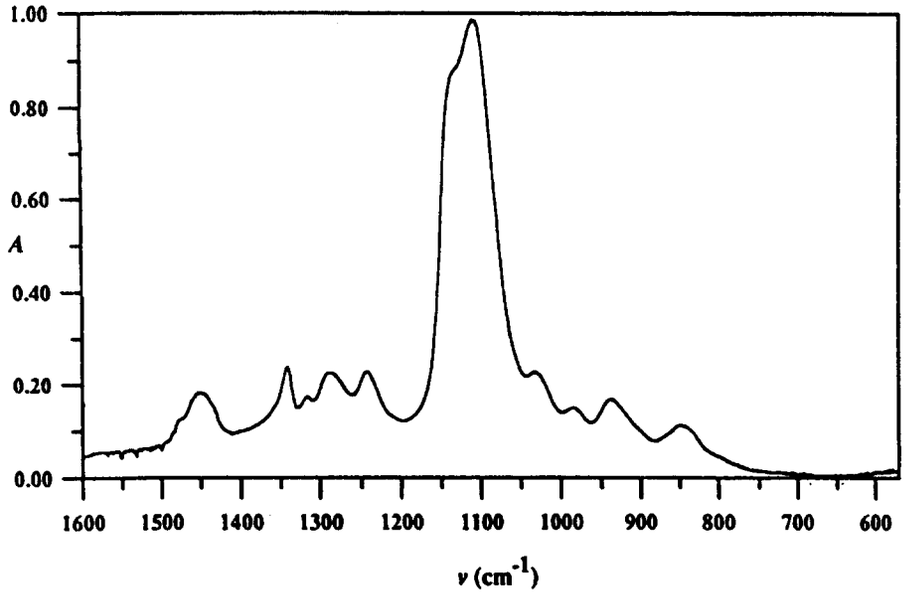

Figure 4 Melt spectrum of PEO, 100°C

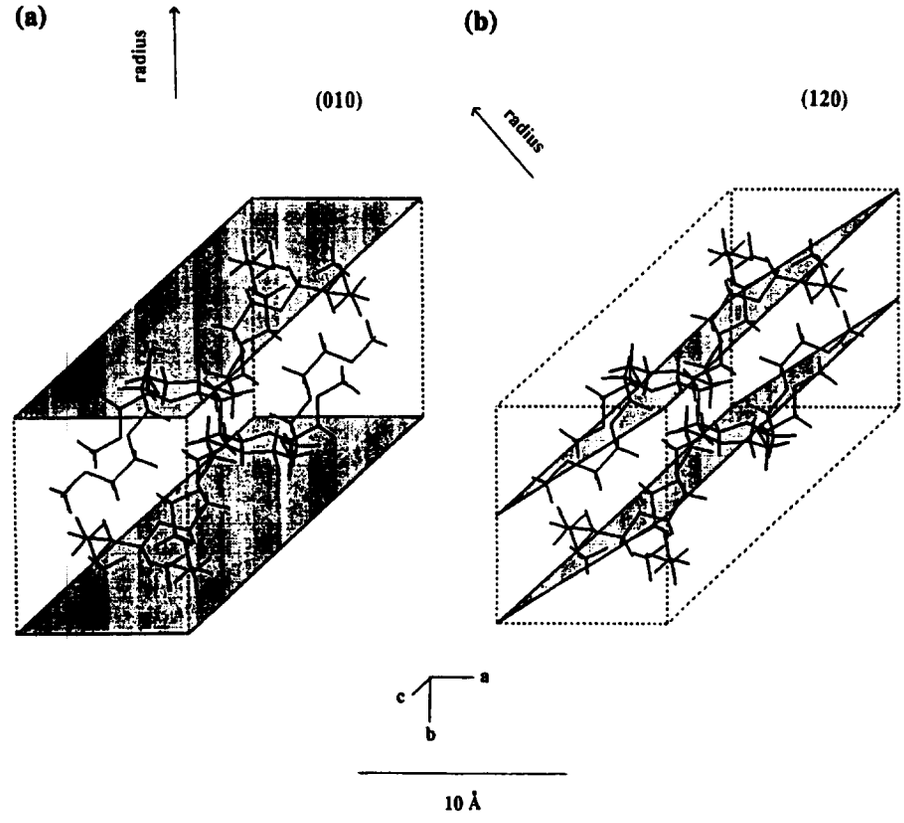

Figure 5 Unit cell diagram of PEO showing the radial direction along with (a) (010) and (b) (120) crystallographic planes

is intended to compensate for the decreasing heat of fusion with decreasing temperature.

If spherulite growth is assumed to proceed via two-dimensional secondary surface nucleation, i.e. new crystalline material is deposited on the surface of the growing spherulite, then the nucleation constant, is given by[25–27]

$$K_g = \frac{2jb_o\sigma\sigma_e T_m^o}{k(\Delta H_f^o)} \quad (4)$$

where b_o is the crystalline molecular thickness in the growth direction, σ is the lateral surface interfacial free energy, σ_e is the fold surface interfacial free energy, T_m^o is the equilibrium melting temperature, and ΔH_f^o is the heat of fusion per unit volume of monomer units. The parameter j depends on the so-called 'regime' of crystallization; it is equal to 2 in regimes I and III, and 1 in regime II.

Radial growth rate data were obtained from spherulites or sectors of spherulites that did not impinge on others during the time span of the measurements. At a given T_c the radial growth rates of at least two spherulites from each of a minimum of three different thin sections were measured to obtain an average growth rate. Typical spherulite sizes ranged from 100 to 1000 μm; and the crystallization time

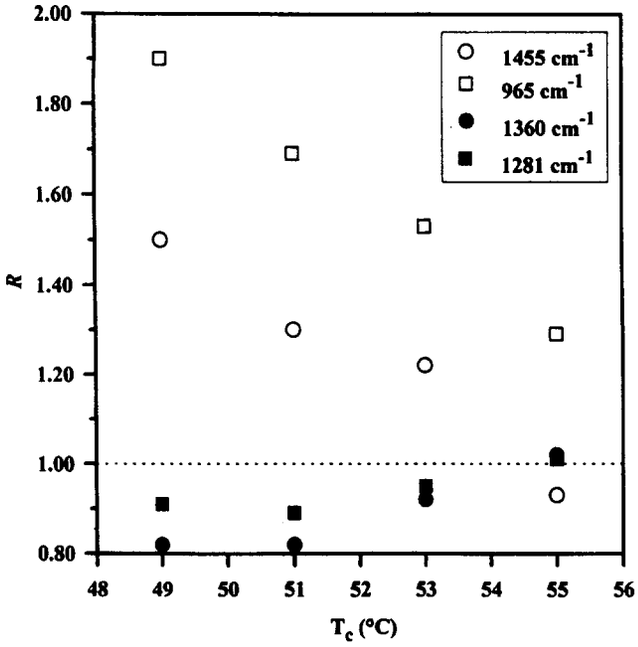

Figure 6 Dichroic ratio as a function of T_c for various parallel (1455 and 965 cm^{-1}) and perpendicular (1360 and 1281 cm^{-1}) modes

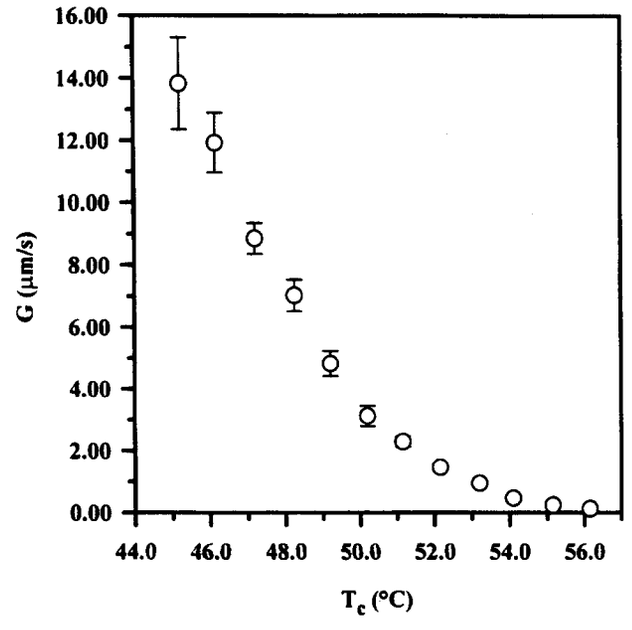

Figure 7 Spherulite radial growth rate, G, of PEO as a function of crystallization temperature, T_c

ranged from 20 s to 3 h. A minimum of eight radius measurements were recorded for each spherulite at a given time to obtain an average value of the radius at that time. Each growth rate was calculated by applying a first order linear regression to a plot of radius as a function of time, with a minimum of five different times. All plots yielded correlation coefficients of better than 0.9990. Radial growth rate as a function of crystallization temperature is plotted in *Figure 7*, with the corresponding logarithmic plot in *Figure 8*. The latter exhibits an apparent cusp, in the vicinity of 51°C, as noted in the literature[1].

The equilibrium melting temperature

An accurate determination of T_m^o is essential to the interpretation of crystallization kinetics data. Various

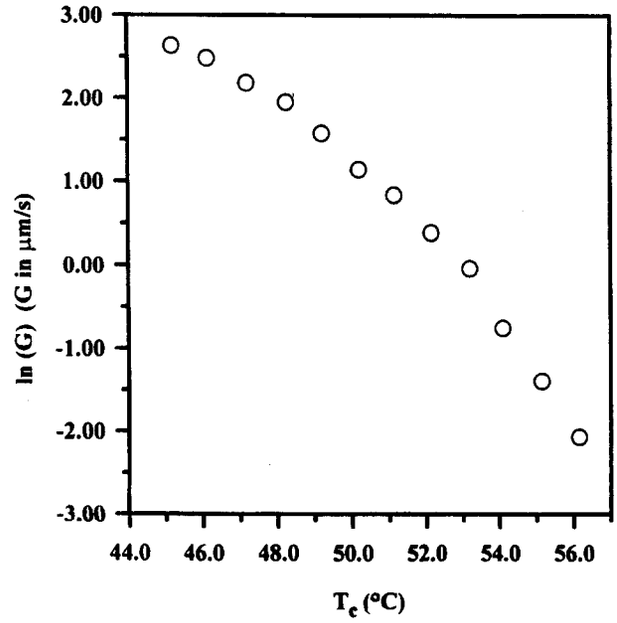

Figure 8 Logarithmic growth rate plot. Note the slight cusp at ~51°C

studies have demonstrated that the values of the parameters in the transport term of equation (2) influence the value of the pre-exponential factor G_o, but have a negligible influence on the ratios of the nucleation constants[25]. On the other hand, the ratios of the nucleation constants, i.e. $K_g(III)/K_g(II)$ and $K_g(I)/K_g(II)$, are very sensitive to the value of T_m^o [25,28,41].

The Hoffman–Weeks (H–W) technique is frequently employed to estimate the value of T_m^o for polymers. It employs the relation[42]

$$T_m = \frac{1}{\eta}T_c + T_m^o\left(1 - \frac{1}{\eta}\right) \quad (5)$$

where η is referred to as the lamellar thickening factor. One requirement is that the values obtained for the observed melting temperature (T_m) correspond to the melting temperatures of the most perfect crystals that can be formed at the chosen values of T_c. Strictly speaking, for this requirement to be upheld the experimental conditions must be selected so as to obtain individual, extended chain crystals. While it may be possible to obtain extended chain crystals of some low molecular weight polymers with a careful choice of conditions[43], with most polymer samples they cannot be obtained, and in practice the most perfect crystals that can be obtained are those formed at early crystallization times and low degrees of crystallinity[44]. However, a further requirement of the H–W technique is that no annealing of the original crystal structure occurs during subsequent heating to determine T_m. In some instances where crystallization is particularly rapid, as in the case of PEO, this requirement can only be satisfied by allowing samples to crystallize to completion at temperatures close to T_m^o, preferably in a temperature range where the lamellar thickening factor is small and constant. In such cases, the re-organization of the crystalline structure on heating is minimal and the resultant T_m approaches the value that would be observed using a sample with a low degree of crystallinity[44].

When the PEO samples used in this study were allowed to crystallize to completion (for periods $\geq$ 24 h) at temperatures from 48 to 59°C, i.e. in the range close to T_m^o which is characterized by a small, constant lamellar

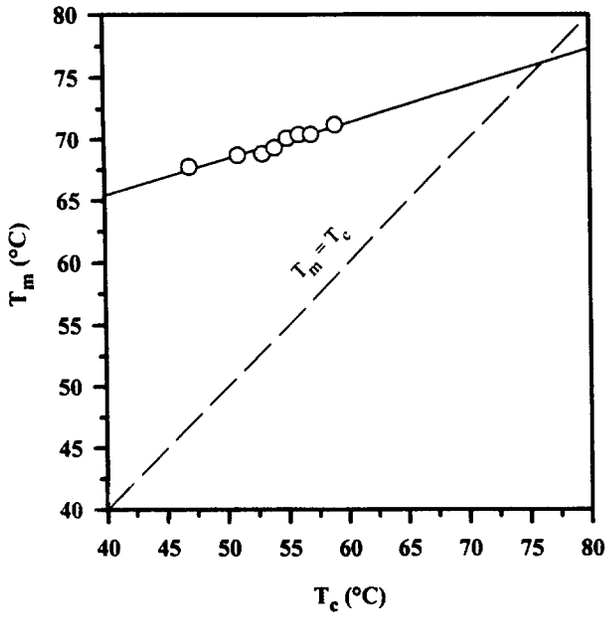

Figure 9 Hoffman–Weeks plot for PEO

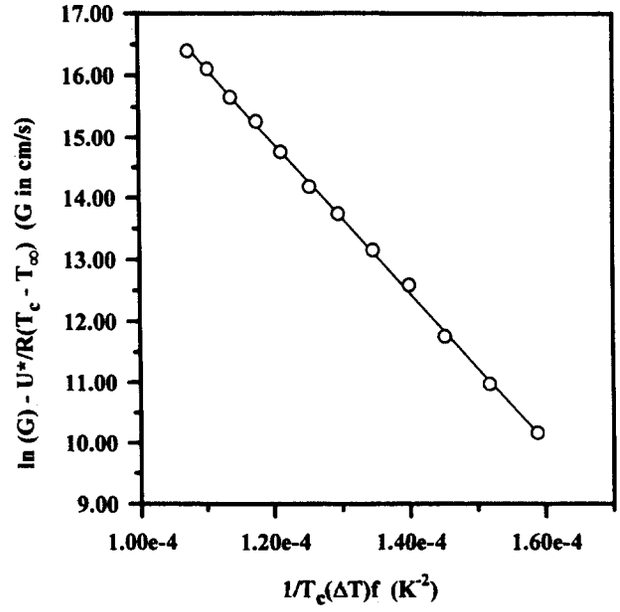

Figure 10 Hoffman–Lauritzen plot

thickening factor, the resultant plot of T_m as a function of T_c yields $T_m^o = 76 \pm 2°C$ (*Figure 9*), where the uncertainty is estimated from the intercept of the plot by linear least squares analysis. This result is in excellent agreement with values of 76 and 75 ± 3°C reported by Beech and Booth[45] and Afifi-Effat and Hay[46], respectively, based on the use of the H–W technique with monodisperse, high molecular weight fractions that were crystallized to low degrees of crystallinity (~10–15%) prior to dilatometry measurements based on slow heating. Alfonso and Russell[20] also reported a value of 76°C using the H–W technique for T_m data obtained by PLM. On the other hand, using an analysis technique developed for molecular crystals by Flory and Vrij[47], Buckley and Kovacs[22] calculated a frequently quoted T_m^o value of 69°C for low molecular weight fractions of PEO. However, Mandelkern later pointed out that these PEO samples could not form molecular crystals[23]; thus, the method of analysis was not applicable. This value is undoubtedly an underestimate, as is evident from the observation that the melting endotherms continue beyond 69°C.

It is important to note that a plot of T_m as a function of T_c for PEO over the extended T_c range 37–59°C is markedly curved. Extrapolation of the different regions of this curve leads to values of T_m^o that span ~15°C, the most probable explanation for the variety of values reported in the literature[22,23]. Extrapolation of an apparently linear segment of the curve that falls in the temperature range ~37–45°C yields a value of ~62°C for T_m^o, a value that is clearly an underestimate given the observed crystallization of PEO at this temperature. In general, curved T_m–T_c plots have been attributed simply to variations in the rate or degree of lamellar thickening with T_c or melting conditions[44,48]. However, in the case of i-PP the curve consists predominantly of two linear segments which correspond closely to the T_c ranges spanned by regimes II and III. Mezghani et al[48] postulated that this behaviour arises ultimately from differences in the crystallization mechanisms in regimes II and III. Similarly, the temperature ranges of the two approximately linear segments of the T_m–T_c plot for PEO appear to reflect the different crystallization mechanisms involved in (010) and (120) growth.

In general, a more appropriate method for the determination of T_m^o is the measurement of the crystal thickness, L, as a function of T_m. However, Alfonso and Russell[20] found that for PEO this is not feasible due to the large dimensions of the crystals and the limited instrument operating range. Therefore, in this instance the H–W technique offers the best available means of evaluating T_m^o.

Radial growth rate data

The growth rate data were evaluated using the Hoffman–Lauritzen equation (equation (2)), with values of −78[30] and 76°C for T_g and T_m^o, respectively. The parameter T_∞ was taken as (T_g − 30 K) or − 108°C. Hoffman[26] has proposed that a 'universal' value of 6.28 kJ/mol for U^* can be applied to most linear polyolefins, but previous studies[1,20,32] have noted that this value appears to be an underestimate for some polymers.

A fit of the growth rate data of the present study according to equation (2) with T_g and T_m^o as constants, and G_o, U^* and K_g as variable parameters yielded an excellent fit ($r = 0.9991$) and a value of U^* of 29.1 kJ/mol. Therefore, the literature value of 29.3 kJ/mol for PEO[22] was accepted for further calculations. The resulting Hoffman–Lauritzen plot, shown in *Figure 10*, is linear (correlation coefficient $r = 0.9996$) and gives no evidence of a change in slope near 51°C, i.e. at the temperature of the cusp seen in *Figure 8*. This suggests that the data fall within a single regime, in accord with previous work by Alfonso and Russell, who studied a PEO sample of a similar molecular weight[20]. Application of the Lauritzen Z-test[25,27,30,49] to the kinetics data suggests that the most probable identity of this regime is regime III, a result that is not surprising given the rapid rates in this T_c range. Thus, it appears that the proposal of a regime II/III transition within this temperature range by Cheng *et al.*[1] results from their choice of a value for T_m^o (69 rather than 76°C). In fact, even for the data obtained in this study the use of $T_m^o = 69°C$ in equation (2) results in a Hoffman–Lauritzen plot with a change in slope at ~51°C; however, the ratio of the slope of the high-T_c segment to that of the low-T_c segment is significantly less than the value of 2 required in the case of a regime II/III transition.

Instead, it appears that the cusp in the logarithmic growth rate–temperature curve (*Figure 8*) reflects a slight shift in the value of the nucleation constant, K_g due to the (010)–(120) growth face transformation. However, this shift must lie within the limits of experimental uncertainty since the change in K_g does not result in a measurable change in the slope of the Hoffman–Lauritzen plot. For the crystallization of PEO the value of K_g derived from the slope of the Hoffman–Lauritzen plot is $(1.22 \pm 0.01) \times 10^5$ K^2, where the uncertainty is as determined from a first-order linear regression using 95% confidence intervals. From K_g, which is equal to $2jb_0\sigma\sigma_e T_m^o/k(\Delta H_f^o)$, the product of the interfacial free energies, $\sigma\sigma_e$, was calculated in the case of each growth face using equation (4) with $\Delta H_f^o = 2.66 \times 10^9$ erg/cm^3 (216 ± 2 J/g)[46,50]; $a_0 = 6.56$ Å and $b_0 = 3.26$ Å for the (010) face; and $a_0 = b_0 = 4.62$ Å for the (120) face[51]. The parameter j was assumed to be equal to 2, as in regime III, due to the relatively low undercooling in the T_c range of interest. Values of 996 and 703 erg^2/cm^4 were obtained for $\sigma\sigma_e$ for the (010) and (120) faces, respectively. Calculation of $\sigma\sigma_e$ with $j = 1$ leads to unreasonably high values for both growth faces, a result that strongly indicates that neither growth face exhibits regime II growth.

The empirical relation[27]

$$\alpha_{LH} = \frac{\sigma}{(\Delta H_f^o)(a_0 b_0)^{1/2}} \quad (6)$$

where a_0b_0 is the cross-sectional area of the polymer, permits estimation of the lateral surface free energy. The parameter α_{LH} is an empirical parameter that has been estimated to be equal to 0.10 for most linear polyolefins[27], while a value of 0.25 ± 0.03 has been found to apply to various high-melting polyesters, such as poly(pivalolactone) (PPVL)[52]. It is likely that the value of α_{LH} for PEO lies between the value for polyolefins such as PE and i-PP (0.10) and that for PPVL. For the purpose of comparison, values of 0.10, 0.15 and 0.20 were used in equation (6) to obtain an estimate of the lateral surface free energy, σ, for PEO; this result was, in turn, used to estimate the fold surface free energy, σ_e (*Table 1*). From the fold surface free energy an additional quantity of interest, the work of chain folding q[26] can be computed from

$$q = 2a_0b_0\sigma_e \quad (7)$$

and is also tabulated. The relative uncertainty in the parameters derived for PEO was estimated at approximately ±10% by taking into account the relative uncertainty in K_g and its components. In the case of literature data, estimates of experimental uncertainty are not available from some sources, but the relative uncertainty can be considered to be approximately the same as in the present study.

In general, $\alpha_{LH} = 0.15$ or 0.20 yields reasonable results relative to available data for other polymers (*Table 2*). In the case of $\alpha_{LH} = 0.20$ the results obtained in this study are similar to those reported by Alfonso and Russell, who assumed a (120) growth face[20]. The product of the interfacial free energies reported by Cheng *et al.*[1], who also assumed a (120) growth face, is based on the assumption of a much lower value of T_m^o and is substantially less than the other values listed for PEO, i-PP and poly(L-lactic acid) (PLLA). However, they noted that re-analysis of their data using a value of 80°C for T_m^o alters the values of K_g and G_o, and yields a value of ~660 erg^2/cm^4 for the product of the interfacial free energies[1], in good agreement with the result obtained for the (120) face in the present study and that obtained for the higher molecular weight fraction of Alfonso and Russell[20].

The interfacial free energy product corresponding to (120) growth in PEO is similar to that of i-PP and PLLA, as expected for a linear polymer that resembles PE. The higher flexibility of the linear PEO as compared with the other, higher melting polymers is manifested in the smaller amount of work required for chain folding. The work of chain folding of PEO is similar to that of another polyether, optically pure poly(epichlorohydrin)[31], but less than that of the less flexible polyester poly(β-hydroxybutyrate) (PHB)[32]. The low value of $\sigma\sigma_e$ for isotactic polystyrene (i-PS) is due to the low surface entropy that results from the relatively rigid chain folds of this aromatic polymer; likewise, the work of chain folding of i-PS is greater than that of the more flexible polymers listed in *Table 2*.

Table 1 Influence of the value of α_{LH} on σ_e and q of PEO ($j = 2$)

	σ_e (erg/cm^2)	q (kJ/mol)
$\alpha_{LH} = 0.10$		
(010)	81	21
(120)	57	15
$\alpha_{LH} = 0.15$		
(010)	54	14
(120)	38	9.8
$\alpha_{LH} = 0.20$		
(010)	41	10
(120)	29	7.4

Table 2 Interfacial free energies and work of chain folding of PEO and various other polymers. (The weight average molecular weight of a given sample is listed in brackets.)

Polymer (MW)	Regime	$\sigma\sigma_e$ (erg^2/cm^4)	σ_e (erg/cm^2)	q (kJ/mol)	T_m^o (°C)	Ref.
PEO (1.45×10^5)	n/a	496	20[a]	5.2[a]	76	20
PEO (5.94×10^5)	n/a	627	26[a]	6.6[a]	76	20
PEO (1.10×10^5)	III	274	14[b]	3.6[b]	69	1
PE	I, II, III	1182 ± 141	94	23	145	25
i-PP	II, III	777 ± 29	68 ± 3	28	185	25
R- or *S*-PECH[c]	III	494	27[d]	7.0[d]	138	31
PHB	II, III	1334	46	21	203	32
PLLA	I, II	733	61	23	207	53
i-PS	II	267	35	30	242	27

[a] σ_e, q not reported, but estimated using $j = 2$, $\alpha_{LH} = 0.20$, (120) growth face
[b] Recalculated from literature data using $\alpha_{LH} = 0.20$
[c] *R*- or *S*-poly(epichlorohydrin)
[d] Estimated from literature data using $\alpha_{LH} = 0.20$

It is perhaps of special interest to compare the interfacial free energy parameters obtained for PEO with those reported for c-PI, since for the latter differences have been observed to occur with a change in the dominant crystal growth face[29]. The different values of σ_e obtained for PEO, and attributed to the two growth faces, are consistent with the distinct change in slope that occurs in the Hoffman–Weeks plot in the vicinity of 51°C. As in the case of c-PI, the structure with higher σ_e melts at significantly lower temperatures than that with lower σ_e. *Cis*-polyisoprene exhibits two distinct crystal types resulting from a change in the dominant crystal growth face, but unlike PEO, both are observed simultaneously over a relatively broad T_c range[29]. The fold surface free energy of the less stable, lower melting, β form of c-PI was determined to be 45 erg/cm^2; while σ_e of the more stable, higher melting, α form was calculated to be 21 erg/cm^2 [29]. This difference in σ_e has been attributed to the longer minimum length required for chain folding in the case of adjacent re-entry in the β lamellae ($a_o = 4.45$ Å, $b_o = 6.23$ Å in α lamellae; $a_o \sim 7.87$ Å, $b_o = 3.62$ Å in β lamellae), with an additional contribution arising from defects in the β structure. The α form was later found to exhibit molecular weight dependent regime transitions[28]; however, σ_e varied only slightly from one regime to another. In the case of PEO, it is important to note that the ratio $\sigma_e(010)/\sigma_e(120)$ is equivalent to the ratio $a_o(010)/a_o(120)$, independent of the value assumed for α_{LH} as seen in *Table 1*. That is, the difference in σ_e of the different growth faces can be accounted for entirely by the difference in the minimum chain length required for adjacent re-entry.

CONCLUSIONS

Polarized infrared microspectroscopy was applied for the first time to the microstructural analysis of local spherulite areas in thin section. This novel technique permitted observation of the occurrence of a transformation in the dominant crystal growth face in PEO spherulites from the (010) crystallographic plane at $T_c < 51$°C to the (120) plane at $T_c > 51$°C. A coarsening of spherulite texture accompanies this transformation. The significance of the use of an accurate value of T_m^o, 76 ± 2°C in the case of PEO, in the analysis of crystallization kinetics data is illustrated by this study. Spherulite radial growth rate data interpreted using Hoffman–Lauritzen theory indicate that crystallization in the T_c range 45–56°C occurs solely within regime III. The nucleation constant, K_g, remains essentially constant in spite of the change in growth face, due to a larger value of $\sigma\sigma_e$ but smaller stem width, b_o, in the case of the (010) growth face. The change in $\sigma\sigma_e$ appears to be due entirely to the change in σ_e. The estimated lateral surface free energy for (010) and (120) growth is constant as a result of the absence of a significant change in the stem area, $a_o b_o$. The differences in σ_e and q of the two growth faces can be accounted for by the difference in the minimum chain length required for chain folding in the case of adjacent re-entry.

ACKNOWLEDGEMENTS

Financial support in the form of operating grants and postgraduate fellowships (JMM) from the Natural Sciences and Engineering Research Council (NSERC), Canada and les Fonds pour la Formation et l'Aide à la Recherche (Fonds FCAR) of Quebec is gratefully acknowledged. The authors also thank Dr Sunil Varshney for the synthesis of the PEO sample, and Mr Ilie Saracovan for aid in preparing unit cell diagrams.

REFERENCES

1. Cheng, S. Z. D., Chen, J. and Janimak, J. J., *Polymer*, 1990, **31**, 1018.
2. Cheng, S. Z. D., Chen, J., Barley, J. S., Zhang, A., Habenschuss, A. and Zschack, P. R., *Macromolecules*, 1992, **25**, 1453.
3. Cheng, S. Z. D., Chen, J., Zhang, A., Barley, J. S., Habenschuss, A. and Zschack, P. R., *Polymer*, 1992, **3**, 1140.
4. Cheng, S. Z. D., Barley, J. S., Chen, J., Habenschuss, A. and Zschack, P. R., *Macromolecules*, 1991, **24**, 3937.
5. Cheng, S. Z. D., Noid, D. W. and Wunderlich, B., *J. Polym. Sci., Polym. Phys. Ed.*, 1989, **27**, 1149.
6. Cheng, S. Z. D., Bu, H. S. and Wunderlich, B., *J. Polym. Sci., Polym. Phys. Ed.*, 1988, **26**, 1947.
7. Cheng, S. Z. D. and Wunderlich, B., *J. Polym. Sci., Polym. Phys. Ed.*, 1986, **24**, 577 and 595.
8. Prud'homme, R. E., *J. Polym. Sci., Polym. Phys. Ed.*, 1982, **20**, 307.
9. Maclaine, J. Q. G. and Booth, C., *Polymer*, 1975, **16**, 680.
10. Price, C., Evans, K. A. and Booth, C., *Polymer*, 1975, **16**, 196.
11. Maclaine, J. Q. G. and Booth, C., *Polymer*, 1975, **16**, 191.
12. Booth, C. and Price, C., *Polymer*, 1966, **7**, 85.
13. Barnes, W. J., Luetzel, W. G. and Price, F. P., *J. Phys. Chem.*, 1961, **65**, 1742.
14. Nakafuku, C. and Sakoda, M., *Polym. J.*, 1993, **25**, 909.
15. Avella, M., Martuscelli, E. and Greco, P., *Polymer*, 1991, **32**, 1647.
16. Quintana, J. R., Cesteros, L. C., Peleteiro, M. C. and Katime, I., *Polymer*, 1991, **32**, 2793.
17. Iragorri, J. I., Cesteros, L. C. and Katime, I., *Polym. Int.*, 1991, **25**, 225.
18. Privalko, V. P., Petrenko, K. D. and Lipatovu, Ye. S., *Polymer*, 1990, **31**, 1277.
19. Margaritis, A. G. and Kalfoglou, N. K., *J. Polym. Sci., Polym. Phys. Ed.*, 1988, **26**, 1595.
20. Alfonso, G. C. and Russell, T. P., *Macromolecules*, 1986, **19**, 1143.
21. Martuscelli, E., Silvestre, C. and Gismondi, C., *Makromol. Chem.*, 1985, **186**, 2161.
22. Buckley, C. P. and Kovacs, A. J., *Progr. Colloid and Polym. Sci.*, 1976, **254**, 695.
23. Mandelkern, L. and Stack, G. M., *Macromolecules*, 1984, **17**, 871.
24. Point, J. J., Damman, P. and Janimak, J. J., *Polymer*, 1993, **34**, 3771.
25. Clark, E. J. and Hoffman, J. D., *Macromolecules*, 1984, **17**, 878.
26. Hoffman, J. D., *Polymer*, 1983, **24**, 3.
27. Lauritzen Jr., J. I. and Hoffman, J. D., *J. Appl. Phys.*, 1973, **44**, 4340.
28. Phillips, P. J. and Vatansever, N., *Macromolecules*, 1987, **20**, 2138.
29. Edwards, B. C., *J. Polym. Sci., Polym. Sci. Ed.*, 1975, **13**, 1387.
30. Marentette, J. M., Ph.D. Thesis, McGill University, Montreal, Canada, 1995.
31. Singfield, K. L. and Brown, G. R., *Macromolecules*, 1995, **28**, 1290.
32. Pearce, R., Brown, G. R. and Marchessault, R. H., *Polymer*, 1994, **35**, 3984.
33. Vidotto, G., Levy, D. and Kovacs, A. J., *Coll. Polym. Sci.*, 1969, **230**, 289.
34. Keith, H. D., Padden Jr, F. J. and Russell, T. P., *Macromolecules*, 1989, **22**, 666.
35. Padden Jr., F. P. and Keith, H. D., *J. Appl. Phys.*, 1959, **30**, 1479.
36. Cheng, S. Z. D., Janimak, J. J. and Zhang, A., *Macromolecules*, 1990, **23**, 298.
37. Lovinger, A. J., Davies, D. D. and Padden Jr., F. P., *Polymer*, 1985, **26**, 1595.
38. Hoffman, J. D., Ross, G. S., Frolen, L. and Lauritzen Jr., J. I., *J. Res. Natl. Bur. Stand., Sect. A*, 1975, **79A**, 671.
39. Koenig, J. L., *Spectroscopy of Polymers*. American Chemical Society, Washington, DC, 1992.
40. Yoshihara, T., Tadokoro, H. and Murahashi, S., *J. Chem. Phys.*, 1964, **41**, 2902.
41. Huang, J., Prasad, A. and Marand, H., *Polymer*, 1994, **35**, 1896.
42. Hoffman, J. D. and Weeks, J. J., *J. Research Natl. Bur. Standards*, 1962, **66A**, 13.
43. Hoffman, J. D., *Polymer*, 1991, **32**, 2828.
44. Alamo, R. G., Viers, B. D. and Mandelkern, L., *Macromolecules*, 1995, **28**, 3205.
45. Beech, D. R. and Booth, C., *Polym. Lett.*, 1970, **8**, 731.

46. Afifi-Effat, A. M. and Hay, J. N., *J. Chem. Soc. Faraday Trans. II*, 1972, **68**, 656.
47. Flory, P. J. and Vrij, A., *JACS*, 1963, **85**, 3548.
48. Mezghani, K., Anderson Campbell, R. and Phillips, P. J., *Macromolecules*, 1994, **27**, 997.
49. Hoffman, J. D., *Polymer*, 1985, **26**, 803.
50. Braun, W., Hellwege, K.-H. and Knappe, W., *Coll. Polym. Sci.* 1967, **215**, 10.
51. Takahashi, Y. and Tadokoro, H., *Macromolecules*, 1973, **6**, 672.
52. Hoffman, J. D., Miller, R. L., Marand, H. and Roitman, D. B. *Macromolecules*, 1992, **25**, 2221.
53. Vasanthakumari, R. and Pennings, A. J., *Polymer*, 1983, **24**, 175.